Wavelet transform on manifolds: old and new approaches

Jean-Pierre Antoine,[a1] Daniela Roşca,[b2] and Pierre Vandergheynst[c3]

[a] *Institut de Physique Théorique, Université catholique de Louvain*
B - 1348 Louvain-la-Neuve, Belgium

[b] *Technical University of Cluj-Napoca, Department of Mathematics*
str. Daicoviciu 15, RO-400020 Cluj-Napoca, Romania

[c] *Signal Processing Institute, Swiss Federal Institute of Technology, EPFL*
Station 11, CH-1015 Lausanne, Switzerland

Abstract

Given a two-dimensional smooth manifold $\mathcal{M}$ and a bijective projection p from $\mathcal{M}$ on a fixed plane (or a subset of that plane), we explore systematically how a wavelet transform (WT) on $\mathcal{M}$ may be generated from a plane WT by the inverse projection p^{-1}. Examples where the projection maps the whole manifold onto a plane include the two-sphere, the upper sheet of the two-sheeted hyperboloid and the paraboloid. When no such global projection is available, the construction may be performed locally, i.e., around a given point on $\mathcal{M}$. We apply this procedure both to the Continuous WT, already treated in the literature, and to the Discrete WT. Finally, we discuss the case of a WT on a graph, for instance, the graph defined by linking the elements of a discrete set of points on the manifold.

1 Introduction

Around 1985, Jean Morlet struggled with the noisy data encountered while prospecting for oil using microseisms. The standard technique was, of course, Fourier transform or better, Short Time Fourier transform. One day he had the brilliant idea of adapting the width of the analysis window to the mean frequency it contains — and it worked! After a thorough collaboration with Alex Grossmann, this purely empirical trick turned into a full-fledged mathematical theory, wavelet analysis was born. Actually, in the founding paper [15], the famous-to-be Morlet wavelet is barely given (one finds only the approximate version "plane wave times Gaussian envelope"). The rest of the story is well-known and most of it, including the original papers, may be found in the compendium [16]: the continuous wavelet transform (CWT), the discrete wavelet transform (DWT), based on the concept of multiresolution analysis, the extension to higher dimension, etc.

Two-dimensional wavelets are by now a standard tool in image processing, under the two concurrent approaches, CWT and DWT. The point is that, while the DWT often leads to wavelet bases, the CWT has to be discretized for numerical implementation and produces in general only frames. However, many situations yield data on *spherical* surfaces. For instance, in Earth and Space sciences (geography, geodesy, meteorology, astronomy, cosmology, etc.), in crystallography (texture analysis of crystals), in medicine (some organs are regarded as sphere-like surfaces), or in computer graphics (modelling of closed surfaces as the graph of a function defined on the sphere). Thus one needs suitable techniques for analyzing such data. In the spherical case, the Fourier transform amounts to an expansion in spherical harmonics, whose support is the whole sphere. Fourier analysis on the sphere is thus global and cumbersome. Therefore many different methods have been proposed to replace it with some sort of wavelet analysis.

[1] *E-mail address*: Jean-Pierre.Antoine@uclouvain.be
[2] *E-mail address*: Daniela.Rosca@math.utcluj.ro
[3] *E-mail address*: pierre.vandergheynst@epfl.ch

In addition, some data may live on more complicated manifolds, such as a *two-sheeted hyperboloid*, in cosmology for instance (an open expanding model of the universe). In optics also, in the catadioptric image processing, where a sensor overlooks a mirror with the shape of a hyperboloid or a *paraboloid*. Another example is a closed sphere-like surface, that is, a surface obtained from a sphere by a smooth deformation. Thus it would be useful to have a wavelet transform available on such manifolds as well.

More generally, we will assume data are given on a two-dimensional smooth manifold $\mathcal{M}$ and we are given a bijective projection p from $\mathcal{M}$ (or a subset $\mathcal{N} \subset \mathcal{M}$) on a plane $\mathbb{R}^2$, for instance a tangent plane or an equatorial plane. We call the projection *global* when it maps the whole manifold bijectively on the plane. Then the idea is to lift WT from $\mathbb{R}^2$ to $\mathcal{M}$ by inverse projection p^{-1}. When no such global projection is available, but only a restricted one, from the subset $\mathcal{N} \subset \mathcal{M}$ to the plane, the analysis may still be performed, but locally. As we will see in the sequel, this method applies both to the CWT and to the DWT. Concrete examples with global projections for $\mathcal{M}$ we have in mind are the two-sphere $\mathbb{S}^2$, the upper sheet of the two-sheeted hyperboloid $\mathbb{H}^2$ and the paraboloid $\mathbb{P}^2$.

The paper is organized as follows. In Section 2, we describe several types of projections from the manifold $\mathcal{M}$ on a plane, stereographic, vertical, conical, radial. Then, in Section 3, we describe the construction of a *global* CWT on $\mathcal{M}$. Here we have to distinguish whether $\mathcal{M}$ admits a global isometry group, as $\mathbb{S}^2$ or $\mathbb{H}^2$, or does not have one, as $\mathbb{P}^2$. In the latter case or more general ones, one can only build a *local* CWT on $\mathcal{M}$, that is, in a (possibly large) neighborhood of a fixed point of $\mathcal{M}$, and this new result is described in Section 4. Here the major difficulty is of (differential) geometrical nature, namely, how to glue together the various local CWTs into a global one. Next, in Section 5, we turn to the case of the DWT and show that, here too, a suitable inverse projection will do the job. Finally, in Section 6, we consider what can be seen as the ultimate discrete manifold, namely, a graph, obtained for instance by linking a given set of points on $\mathcal{M}$, and show how to design a WT on it. As far as we know, such a construction has not been proposed in the literature.

2 Preliminaries: Geometry of projections

Let $\mathcal{M}$ be a C^1 -surface defined by the equation $\zeta = \zeta(\mathbf{x}) = (\zeta_1(x,y), \zeta_2(x,y), \zeta_3(x,y))$, $\mathbf{x} = (x,y) \in D \subseteq \mathbb{R}^2$. We consider the function $J : D \to \mathbb{R}$,

$$J(x,y) = \left| \frac{\partial \zeta}{\partial x} \times \frac{\partial \zeta}{\partial y} \right|.$$

Let $\mathsf{p} : \mathcal{M} \to D$ denote the projection of the surface $\mathcal{M}$ onto the plane Oxy, that is

$$\mathsf{p}(\zeta_1(x,y), \zeta_2(x,y), \zeta_3(x,y)) = (x,y), \text{ for all } (x,y) \in D.$$

This projection is bijective and its inverse is obviously

$$\mathsf{p}^{-1} : D \to \mathcal{M},\ \mathsf{p}^{-1}(x,y) = (\zeta_1(x,y), \zeta_2(x,y), \zeta_3(x,y)).$$

The projection p is global if $D = \mathbb{R}^2$, local if D is a proper subset of $\mathbb{R}^2$. The relations between $d\mathbf{x} = dx\, dy$, the area element of $\mathbb{R}^2$, and $d\mu(\zeta)$, the area element of $\mathcal{M}$, are

$$\begin{aligned} d\mu(\zeta) &= J(\mathbf{x})\, d\mathbf{x}, \\ d\mathbf{x} &= \frac{1}{(J \circ \mathsf{p})(\zeta)} d\mu(\zeta), \text{ where } \zeta = (\zeta_1, \zeta_2, \zeta_3) \in \mathcal{M}. \end{aligned}$$

In $L^2(\mathcal{M})$ we define the scalar product $\langle\cdot,\cdot\rangle_*$ as

$$\langle\mathcal{F},\mathcal{G}\rangle_* = \langle\mathcal{F}\circ\mathsf{p}^{-1},\mathcal{G}\circ\mathsf{p}^{-1}\rangle_{L^2(D)}, \text{ for all } \mathcal{F},\mathcal{G}\in L^2(\mathcal{M}). \tag{2.1}$$

If we consider the function $\nu:\mathcal{M}\to\mathbb{R},\ \nu=(J\circ\mathsf{p})^{-1/2}$, then one has

$$\begin{aligned}\langle\mathcal{F},\mathcal{G}\rangle_* &= \int_D \overline{\mathcal{F}(\mathsf{p}^{-1}(x,y))}\,\mathcal{G}(\mathsf{p}^{-1}(x,y))\,dx\,dy\\ &= \int_{\mathcal{M}} \overline{\mathcal{F}(\zeta)}\,\mathcal{G}(\zeta)\,\nu^2(\zeta)\ d\mu(\zeta).\end{aligned}$$

Thus, the scalar product $\langle\cdot,\cdot\rangle_*$ is a weighted scalar product, with the weight function ν^2.

On the other hand, if $F,G\in L^2(D)$ are given, then

$$\langle F,G\rangle_{L^2(D)} = \int_D \overline{F(\mathbf{x})}\,G(\mathbf{x})\,d\mathbf{x} = \int_{\mathcal{M}} \overline{F(\mathsf{p}(\zeta))}\,G(\mathsf{p}(\zeta))\nu^2(\zeta)d\mu(\zeta),$$

which means that

$$\langle F,G\rangle_{L^2(D)} = \langle\nu\cdot(F\circ\mathsf{p}),\nu\cdot(G\circ\mathsf{p})\rangle_{L^2(\mathcal{M})}, \tag{2.2}$$

or, using the definition (2.1), one can write

$$\langle F\circ\mathsf{p},G\circ\mathsf{p}\rangle_* = \langle F\circ\mathsf{p}\circ\mathsf{p}^{-1},G\circ\mathsf{p}\circ\mathsf{p}^{-1}\rangle_{L^2(D)} = \langle F,G\rangle_{L^2(D)}. \tag{2.3}$$

In other words, the map

$$\pi^{-1}: F\mapsto\mathcal{F}:=\nu\cdot(F\circ\mathsf{p}) \tag{2.4}$$

is unitary from $L^2(D)$ onto $L^2(\mathcal{M})$ and, similarly, the map $F\mapsto F\circ\mathsf{p}$ from $L^2(D)$ onto $L^2(\mathcal{M},*)$, i.e., $\mathcal{M}$ with the scalar product (2.1). In particular, this implies that, if the functions $F,G\in L^2(D)$ are orthogonal with respect to the usual scalar product of $L^2(D)$, then:

- $\nu\cdot(F\circ\mathsf{p})\in L^2(\mathcal{M}),\ \nu\cdot(G\circ\mathsf{p})\in L^2(\mathcal{M})$ and they are orthogonal with respect to the usual scalar product of $L^2(\mathcal{M})$;
- $F\circ\mathsf{p}\in L^2(\mathcal{M}),\ G\circ\mathsf{p}\in L^2(\mathcal{M})$ and they are orthogonal with respect to the weighted scalar product defined in (2.1).

These facts will allow us to use any orthogonal wavelet basis defined on D in order to construct an orthogonal wavelet basis defined on the manifold $\mathcal{M}$.

An important property of the scalar product $\langle\cdot,\cdot\rangle_*$ is given in the next proposition.

Proposition 2.1 *If there exist* $\mathsf{m},\mathsf{M}\in(0,\infty)$ *such that*

$$\mathsf{m}\leqslant\nu(\zeta)\leqslant\mathsf{M},\ \textit{for all } \zeta\in\mathcal{M}, \tag{2.5}$$

then the norm $\|\cdot\|_*=\langle\cdot,\cdot\rangle_*^{1/2}$*, induced by the scalar product* $\langle\cdot,\cdot\rangle_*$*, is equivalent to the usual 2-norm of* $L^2(\mathcal{M})$*.*

Proof. It is immediate that

$$\mathsf{m}^2\mathcal{F}^2(\zeta)\leqslant\nu^2(\zeta)\mathcal{F}^2(\zeta)\leqslant\mathsf{M}^2\mathcal{F}^2(\zeta),$$

for all $\zeta=(\zeta_1,\zeta_2,\zeta_3)\in\mathcal{M}$. Thus, integrating on $\mathcal{M}$, we obtain

$$\mathsf{m}\|\mathcal{F}\|_2\leqslant\|\mathcal{F}\|_*\leqslant\mathsf{M}\|\mathcal{F}\|_2.$$

$\square$

Now we consider some particular cases. If the manifold $\mathcal{M}$ is a surface of revolution and the projection p conserves the longitude, it is more natural to use polar coordinates $\zeta=(s,\varphi)$ on $\mathcal{M}$, with $\varphi\in[0,2\pi)$, the longitude angle, and s a coordinate along the section $\varphi=$ const. Then, in planar polar coordinates (r,φ), the projection reads $\mathsf{p}(\zeta)=\mathsf{p}(s,\varphi)=(r(s),\varphi)$.

2.1 The stereographic projection

(a) Stereographic projection of the two-sphere

With the notations in Section 2, let $\mathcal{M}$ be the pointed two-sphere $\dot{\mathbb{S}}^2 = \{(\zeta_1, \zeta_2, \zeta_3) \in \mathbb{R}^3,\ \zeta_1^2 + \zeta_2^2 + (\zeta_3 - 1)^2 = 1\} \setminus \{(0,0,2)\}$ and let $\mathsf{p} : \mathcal{M} \to \mathbb{R}^2$ be the stereographic projection from the North Pole $N(0,0,2)$ onto the tangent plane at the South Pole. If we take polar coordinates $\zeta = (\theta, \varphi)$, where $s = \theta \in [0, \pi)$ is the colatitude and $\varphi \in [0, 2\pi)$ is the longitude, then the stereographic projection is given by $r(\theta) = 2\tan\frac{\theta}{2}$, and it is the only longitude preserving projection that is conformal [33].

Then one can easily see that

$$\nu(\zeta) = \frac{2}{2 - \zeta_3} = \frac{1}{\sin^2\frac{\theta}{2}}\,,$$

and this function does not satisfy the condition (2.5) in Proposition 2.1. The relations between ζ and $\mathbf{x} = \mathsf{p}(\zeta)$ are

$$x = \zeta_1\, \nu(\zeta),\ \ y = \zeta_2\, \nu(\zeta),$$

and

$$\zeta_1 = x\ \varrho(\mathbf{x}),\ \ \zeta_2 = y\ \varrho(\mathbf{x}),\ \ \zeta_3 = \frac{1}{2}(x^2 + y^2)\varrho(\mathbf{x}),$$

with $\varrho(\mathbf{x}) = 4(x^2 + y^2 + 4)^{-1}$. Yet we still have a unitary map between $L^2(\mathbb{R}^2)$ and $L^2(\dot{\mathbb{S}}^2)$.

(b) Stereographic projection of the two-sheeted hyperboloid

Consider the upper sheet $\mathbb{H}^2_+$ of the two-sheeted hyperboloid $\mathbb{H}^2$, given by the explicit equation

$$\zeta_3 = \sqrt{1 + \zeta_1^2 + \zeta_2^2}.$$

The stereographic projection from the South Pole of $\mathbb{H}^2$ maps the upper sheet $\mathbb{H}^2_+$ onto the open unit disk in the equatorial plane $\zeta_3 = 0$ (it maps the lower sheet onto the exterior of the unit disk). In terms of polar coordinates $\zeta = (\chi, \varphi)$, where $\chi \geqslant 0$ and $\varphi \in [0, 2\pi)$ is the longitude, the stereographic projection is given by $r(\chi) = \tanh\frac{\chi}{2}$. Then a direct computation yields

$$\nu(\zeta) = \nu(\chi, \varphi) = \frac{1}{2\cosh^2\frac{\chi}{2}}.$$

Thus one has $0 \leqslant \nu(\zeta) \leqslant \frac{1}{2}$ and condition (2.5) is not satisfied.

2.2 The vertical projection

Suppose that the surface $\mathcal{M}$ is given by the explicit equation $z = f(\mathbf{x})$, $\mathbf{x} = (x, y) \in D \subseteq \mathbb{R}^2$. In this case we consider the vertical projection $\mathsf{p} : \mathcal{M} \to D$,

$$\mathsf{p}(x, y, f(x, y)) = (x, y),\ \text{for all } (x, y) \in D.$$

The function ν is

$$\nu = \left[1 + \left(\frac{\partial f}{\partial x}\right)^2 + \left(\frac{\partial f}{\partial y}\right)^2\right]^{-1/4}$$

and the relations between $\zeta = (\zeta_1, \zeta_2, \zeta_3) \in \mathcal{M}$ and $(x, y) = \mathsf{p}(\zeta)$ are

$$x = \zeta_1,\ \ y = \zeta_2$$

and

$$\zeta_1 = x,\ \zeta_2 = y,\ \zeta_3 = f(x, y).$$

(a) Vertical projection of the two-sphere

Let $\mathcal{M}$ be a unit sphere centered in $(0, 0, 1)$. Then the two hemispheres obey the equations

$$z = 1 \pm \sqrt{1 - x^2 - y^2}.$$

Obviously the corresponding function ν does not satisfy the condition (2.5).

(b) Vertical projection of the hyperboloid

Consider again the upper sheet of the (general) two-sheeted hyperboloid, given by the explicit equation

$$z = c\sqrt{1 + \frac{x^2}{a^2} + \frac{y^2}{b^2}}$$

(the normalized case $\mathbb{H}^2_+$ correspond to $a = b = c = 1$). The calculation shows that

$$\nu(\zeta) = \left(1 + \frac{c^2}{a^2b^2} \cdot \frac{b^4\zeta_1^2 + a^4\zeta_2^2}{b^2\zeta_1^2 + a^2\zeta_2^2 + a^2b^2}\right)^{-1/4}$$

and condition (2.5) is satisfied with

$$M = 1,\ m = \left(1 + \frac{c^2}{\min\{a^2, b^2\}}\right)^{-1/4}$$

For the normalized case $\mathbb{H}^2_+$, the vertical projection yields $r(\chi) = \sinh\chi$ and

$$\nu(\zeta) = \left(1 + \tanh^2\frac{\theta}{2}\right)^{-1/4}.$$

(c) Vertical projection of the paraboloid

Consider the elliptic paraboloid with explicit equation

$$z = \frac{x^2}{a^2} + \frac{y^2}{b^2}.$$

Simple calculations show that

$$\nu(\zeta) = \frac{ab}{\left(4b^4\zeta_1^2 + 4a^4\zeta_2^2 + a^4b^4\right)^{1/4}}$$

and obviously the function ν does not satisfy condition (2.5) in Proposition 2.1.

2.3 The conical projection of the hyperboloid

In the case of the two-sheeted hyperboloid $\mathbb{H}^2_+$, an alternative consists in projecting it first on its tangent half null-cone

$$\mathcal{C}^2_+ = \{\mathbf{x} = (z, x, y) \in \mathbb{R}^3 : z^2 - x^2 - y^2 = 0,\ z > 0\},$$

then vertically on the plane $z = 0$. The result is $r(\chi) = 2\sinh\frac{\chi}{2}$. In fact, there is an infinite family of projections from $\mathbb{H}^2_+$ onto the plane $z = 0$, leading to $r(\chi) = \frac{1}{p}\sinh p\chi$, but the case $p = \frac{1}{2}$ seems the most natural one. More details may be found in [5, 7, 9].

The same technique can be used for the one-sheeted hyperboloid $\mathbb{H}^{1,1}$, of equation $z^2 = -1 + x^2 + y^2$, which has the same tangent null-cone $\mathcal{C}^2 = \{\mathbf{x} = (z, x, y) \in \mathbb{R}^3 : z^2 - x^2 - y^2 = 0\}$.

2.4 Radial projection from a convex polyhedron onto the sphere

A variant of the preceding constructions consists in projecting radially the faces of a convex polyhedron onto the sphere [23, 27]. Let $\mathbb{S}^2$ be the unit sphere centered in 0 and let Γ be a convex polyhedron, containing 0 in its interior and with triangular faces (if some faces are non-triangular, one simply triangularizes them). Let $\Omega = \partial\Gamma$ denote the boundary of Γ and let $p : \Omega \to \mathbb{S}^2$ denote the radial projection from the origin:

$$p(x, y, z) = \rho \cdot (x, y, z), \qquad \text{where } \rho := \rho(x, y, z) = 1/\sqrt{x^2 + y^2 + z^2}.$$

Let $\mathcal{T}$ denote the set of triangular faces of Γ and consider the following weighted scalar product on $L^2(\mathbb{S}^2)$:

$$\langle F, G\rangle_\Gamma = \sum_{T\in\mathcal{T}} \int_{p(T)} F(\zeta)\, G(\zeta)\, w_T(\zeta)\, d\mu(\zeta), \quad \zeta = (\zeta_1, \zeta_2, \zeta_3) \in \mathbb{S}^2,\ F, G \in L^2(\mathbb{S}^2).$$

Here $w_T(\zeta_1, \zeta_2, \zeta_3) = 2d_T^2\, |a_T\zeta_1 + b_T\zeta_2 + c_T\zeta_3|^{-3}$, with a_T, b_T, c_T, d_T the coefficients of $x, y, z, 1$, respectively, in the determinant

$$\begin{vmatrix} x & y & z & 1 \\ x_1 & y_1 & z_1 & 1 \\ x_2 & y_2 & z_2 & 1 \\ x_3 & y_3 & z_3 & 1 \end{vmatrix} = a_T x + b_T y + c_T z + d_T 1,$$

where (x_i, y_i, z_i), $i = 1, 2, 3$, are the vertices of the planar triangle $T \in \mathcal{T}$. Then, as in the case of condition (2.5) in Proposition 2.1, one proves that the norm $\|\cdot\|_\Gamma := \langle\cdot,\cdot\rangle_\Gamma^{1/2}$ is equivalent to the usual norm in $L^2(\mathbb{S}^2)$, i.e., there exist constants $\mathsf{m}_\Gamma > 0$, $\mathsf{M}_\Gamma < \infty$ such that

$$\mathsf{m}_\Gamma \,\|f\|_\Gamma \leqslant \|f\|_2 \leqslant \mathsf{M}_\Gamma \,\|f\|_\Gamma\,,\ \forall\, f \in L^2(\mathbb{S}^2).$$

Explicit expressions for optimal bounds m_Γ and M_Γ are given in [28].

3 Constructing a global CWT on the manifold $\mathcal{M}$

In order to build a CWT on the manifold $\mathcal{M}$, one starts by identifying the operations one wants to perform on the finite energy signals living on $\mathcal{M}$, that is, functions in $L^2(\mathcal{M}, d\mu)$, where μ is a suitable measure on $\mathcal{M}$. Next one realizes these operations by unitary operators on $L^2(\mathcal{M}, d\mu)$. Mimicking the flat case, the required transformations are of two types: (i) *motions*, which are realized by isometries of $\mathcal{M}$, and (ii) *dilations* of some sort by a scale factor $a > 0$. In addition, one may look for a possible group-theoretical derivation.

For motions, we may distinguish two cases, depending whether $\mathcal{M}$ admits a global isometry group or not. As for dilations, the problem is how to define properly them *on* the manifold $\mathcal{M}$ itself. One possibility is to lift them, by an inverse projection, from dilations in a tangent plane or cone, that is, the dilation on $\mathcal{M}$ is defined as

$$D_a^{(\mathcal{M})} : \mathsf{p}^{-1} \circ d_a \circ \mathsf{p}, \tag{3.1}$$

where p is the projection of $\mathcal{M}$ on the plane or cone and d_a is the known dilation on the latter.

3.1 $\mathcal{M}$ with global isometry group

In the first class, manifolds which admit a global isometry group, we find the two-sphere $\mathbb{S}^2$ and the two-sheeted hyperboloid. Their isometry group are the (compact) rotation group SO(3) and the (noncompact) Lorentz-type group $\mathrm{SO}_o(2,1)$, respectively.

(a) The two-sphere $\mathbb{S}^2$

The construction of a CWT on the two-sphere $\mathbb{S}^2$ with help of the stereographic projection has been thoroughly treated in the literature [1, 3, 4], so we just quote the results.

(1) The spherical CWT of a function $f \in L^2(\mathbb{S}^2, d\mu)$ with respect to the (admissible) wavelet ψ is defined as

$$W_f(\varrho, a) := \langle \psi_{\varrho,a}, f \rangle = \int_{\mathbb{S}^2} \overline{\psi_a(\varrho^{-1}\zeta)}\, f(\zeta)\, d\mu(\zeta), \ \ \varrho \in \mathrm{SO}(3), a > 0, \tag{3.2}$$

where μ is the usual rotation invariant measure on $\mathbb{S}^2$ and $\psi_a(\zeta) := \lambda(a,\theta)^{1/2}\psi(\zeta_{1/a})$, $a > 0$. In these relations, $\zeta_a = (\theta_a, \varphi)$, θ_a is defined by $\cot\frac{\theta_a}{2} = a\cot\frac{\theta}{2}$ for $a > 0$ and the normalization factor $\lambda(a,\theta)^{1/2}$ (Radon-Nikodym derivative) is needed for compensating the noninvariance of the measure μ under dilation. Clearly the operator $f(\zeta) \mapsto f(\zeta_{1/a})$ is built on the model (3.1), with p the stereographic projection.

(2) The transform (3.2) has all the properties of the plane CWT: exact inversion (reconstruction formula), reproducing kernel, etc. In addition, it has a correct Euclidean limit. That is, if we construct the transform on a sphere of radius R and then let $R \to \infty$, the spherical CWT tends to the usual plane 2-D CWT on the tangent plane at the South Pole.

(3) The transform (3.2) can be obtained by a group-theoretical derivation (the so-called coherent state method), using the Lorentz group $\mathrm{SO}_o(3,1)$ (which is the conformal group both of $\mathbb{S}^2$ and of its tangent plane $\mathbb{R}^2$).

(4) The unitary map π^{-1} defined in (2.4) allows to generate a spherical wavelet $\pi^{-1}(\psi)$ from any plane 2-D wavelet ψ. Examples are the familiar Mexican hat, Difference-of-Gaussians, and Morlet wavelets. The latter, in particular, behaves on the sphere exactly as its plane counterpart does on the plane [3].

(5) Discretization of the spherical CWT leads to various types of (generalized) frames, either half-continuous (only the scale variable is discretized) or fully discrete. Technical details may be found in [8].

(b) The two-sheeted hyperboloid $\mathbb{H}^2$

This case is entirely parallel to the previous one, replacing SO(3) by the isometry group $\mathrm{SO}_o(2,1)$, the elements of which are of two types: (i) rotations : $x(\chi,\varphi) \mapsto (\chi, \varphi+\varphi_0)$; and (ii) hyperbolic motions : $x(\chi,\varphi) \mapsto (\chi+\chi_0, \varphi)$. As for dilations, a choice has to be made, each type being defined by one of the available projections described above. Details may be found in [7, 9].

(1) Given an (admissible) hyperbolic wavelet ψ, the hyperbolic CWT of $f \in L^2(\mathbb{H}^2_+)$ with respect to ψ is

$$\mathcal{W}_f(g,a) := \langle \psi_{g,a}, f\rangle = \int_{\mathbb{H}^2_+} \overline{\psi_a(g^{-1}\zeta)}\, f(\zeta)\, d\mu(\zeta),\; g \in \mathrm{SO}_o(2,1), a>0. \tag{3.3}$$

As in the spherical case, $\psi_a(x) = \lambda(a,\zeta)\psi(d_{1/a}\zeta)$, with d_a an appropriate dilation, and $\lambda(a,x)$ is the corresponding Radon-Nikodym derivative, and μ is the $\mathrm{SO}_o(2,1)$-invariant measure on $\mathbb{H}^2$. Once again, this operation is built on the model (3.1).

(2) The key for developing the CWT is the possibility of performing harmonic analysis on $\mathbb{H}^2_+$, including a convolution theorem, thanks to the so-called Fourier-Helgason transform. As a consequence, the usual properies hold true, for instance,an exact reconstruction formula.

(3) However, no result is known concerning frames that would be obtained by discretization.

(c) The one-sheeted hyperboloid $\mathbb{H}^{1,1}$

The same analysis can be made for the one-sheeted hyperboloid $\mathbb{H}^{1,1}$, since it has the same isometry group $\mathrm{SO}_o(2,1)$, the same tangent null-cone $\mathcal{C}^2$, hence the same type of conical projections, and a Fourier-Helgason-type transform with the required properties [6, 10].

3.2 $\mathcal{M}$ without global isometry group

If the manifold $\mathcal{M}$ does not admit a global isometry group, the previous method cannot be used. A case in point is the axisymmetric paraboloid $\mathbb{P}^2$, of equation $z = x^2+y^2$. A group-theoretical tentative exists [19], based on a homeomorphim from a cylinder onto the pointed paraboloid $\dot{\mathbb{P}}^2 := \mathbb{P}^2 \setminus \{0\}$, but it does not produce convincing results, in particular, the formalism does not allow for a local dilation around an arbitrary point. Some additional details may be found in [5].

This being so, an alternative consists in lifting the wavelets from the tangent plane at the origin onto $\mathbb{P}^2$, using the inverse vertical projection. Another one is to define a *local* wavelet transform, as explained in the next section in the case of a general manifold.

4 CWT on a general manifold: Local wavelet transform

For simplicity, we continue to assume that $\mathcal{M}$ is a smooth 2-D surface. However, the analysis extends easily to a smooth manifold of arbitrary dimension n. Let $\mathfrak{H} = L^2(\mathcal{M}, d\mu)$ be the Hilbert space of square-integrable functions on $\mathcal{M}$, for a proper measure $d\mu$, with scalar product $\langle\cdot,\cdot\rangle_{\mathfrak{H}}$. In the following $T_\zeta(\mathcal{M})$ will denote the tangent space at $\zeta \in \mathcal{M}$.

Our construction is entirely local and rooted in differential geometry. At any point $\zeta \in \mathcal{M}$, we start by constructing a prototype wavelet. Generally speaking, this is a square integrable function $\psi^{(\zeta)} \in \mathfrak{H}$ that is compactly supported in a neighborhood $\mathcal{B}_\zeta$ of $\zeta \in \mathcal{M}$. The size of $\mathcal{B}_\zeta$ will depend on the local geometry of $\mathcal{M}$. The second step is to define a suitable local dilation operator. In order to exploit dilations in $\mathbb{R}^n$, we will equip $\mathcal{M}$ with a local Euclidean structure by mapping $\mathcal{B}_\zeta$ to $T_\zeta(\mathcal{M})$. A simple way to implement this mapping is by *flattening* $\mathcal{B}_\zeta$ along the normal to $\mathcal{M}$ at ζ. Let p_ζ be that local flattening map:

$$\mathsf{p}_\zeta : \mathcal{B}_\zeta \mapsto T_\zeta(\mathcal{M}). \tag{4.1}$$

In order for that mapping to be useful, we choose the size of $\mathcal{B}_\zeta$ such that p_ζ is a diffeomorphism.

Let $\alpha \in \mathcal{B}_\zeta$. A local dilation of coordinates is defined as in (3.1):

$$\alpha \mapsto \alpha_a = \mathsf{p}_\zeta^{-1} \circ a \circ \mathsf{p}_\zeta(\alpha). \tag{4.2}$$

Obviously, the definition of p_ζ sets a local maximum scale $a_{\max}^{(\zeta)}$ so that (4.2) is well-defined.

We can now easily construct a dilation operator acting on functions with support in $\mathcal{B}_\zeta$. For convenience, we will denote by $\mathfrak{H}(\mathcal{B}_\zeta)$ this subspace of $\mathfrak{H}$. Given $\psi^{(\zeta)} \in \mathfrak{H}(\mathcal{B}_\zeta)$, the following operator maps $\mathfrak{H}(\mathcal{B}_\zeta)$ unitarily to itself:

$$D_\zeta(a) : \psi^{(\zeta)}(\alpha) \mapsto \lambda^{1/2}(a,\alpha)\psi^{(\zeta)}(\alpha_{a^{-1}}),$$

where, as usual,

$$\lambda(a,\alpha) = \frac{d\mu(\alpha_{a^{-1}})}{d\mu(\alpha)}$$

is the corresponding Radon-Nikodym derivative that takes care of the possible noninvariance of the measure μ under dilation. For the sake of compactness, we will use the shorter notation $\psi_a^{(\zeta)} := D_\zeta(a)\psi^{(\zeta)}$. Note that, by construction, D_ζ will be continuous as a function of ζ provided the normal to $\mathcal{M}$ at ζ varies smoothly.

Given a signal $f \in \mathfrak{H}$, we can now define its wavelet transform at $\zeta \in \mathcal{M}$ and scale a as

$$\mathcal{W}_f(\zeta, a) = \langle \psi_a^{(\zeta)}, f \rangle_{\mathfrak{H}}. \tag{4.3}$$

The inverse transform will take the general form:

$$f = \int_{\mathcal{M}} d\mu(\zeta) \int_0^{a_\psi(\zeta)} \frac{da}{a^\beta}\, \mathcal{W}_f(\zeta, a)\, \psi_a^{(\zeta)}.$$

The bound $a_\psi(\zeta)$ used in this formula is a cut-off ensuring that the support of the dilated wavelet $\psi_{a_\psi(\zeta)}^{(\zeta)}$ stays under control, i.e., $\mathrm{supp}(\psi_{a_\psi(\zeta)}^{(\zeta)}) \subset \mathcal{B}_\zeta$. As for the exponent β, it depends on the manifold at hand and serves the same purpose.

4.1 The case of the circle

As an example of the preceding construction, but in dimension 1, we take the case where $\mathcal{M} = \mathbb{S}^1$, the unit circle in $\mathbb{R}^2$ and perform the calculation explicitly. The same calculation will then yield the CWT on the two-sphere generated by the vertical projection.

4.1.1 Construction of local dilations

In this case, $\mathfrak{H} = L^2(\mathbb{S}^1, d\alpha)$ and ζ is the angle $\varphi \in \mathbb{S}^1$. A simple calculation shows that the flattening map (4.1) has the following explicit form:

$$\mathsf{p}_\varphi(\alpha) = \sin(\alpha - \varphi).$$

Obviously, p_φ coincides with the vertical projection defined in Section 2.2(a). In particular, for $\varphi = -\pi/2$ (the South "Pole"), $\mathsf{p}_{-\pi/2}(\alpha) = \cos\alpha$, as it should.

This operation is defined in a neighborhood of size π centered on φ, i.e., $\mathcal{B}_\varphi = [\varphi - \pi/2, \varphi + \pi/2]$. A dilation of coordinates around φ will then be given by

$$\alpha \mapsto \alpha_a = \arcsin\big(a \sin(\alpha - \varphi)\big) + \varphi, \quad a > 0, \tag{4.4}$$

and the maximum local dilation that can be applied to a point α is $a_{\max} = |\sin(\alpha - \varphi)|^{-1}$.

In order to define the dilation operator acting on $\mathfrak{H}(\mathcal{B}_\varphi)$, we first compute the Radon-Nikodym derivative:

$$\lambda(a, \alpha) = \frac{d\alpha_{a^{-1}}}{d\alpha} = \frac{\cos(\alpha - \varphi)}{\sqrt{a^2 - \sin^2(\alpha - \varphi)}}.$$

It is easy to check that indeed it satisfies a cocycle relation: $\lambda^{-1}(a, \alpha_a)\lambda(a, \alpha) = 1$. If $\psi^{(\varphi)}$ is a bounded function compactly supported in $[\varphi - \Delta, \varphi + \Delta] \subset \mathcal{B}_\varphi$, we have

$$\psi_a^{(\varphi)}(\alpha) = \lambda(a, \alpha)^{1/2}\, \psi^{(\varphi)}(\alpha_{a^{-1}}), \tag{4.5}$$

and the maximal dilation applicable to the wavelet $\psi^{(\varphi)}$ is

$$a_\psi(\varphi) = |\sin(\varphi + \Delta - \varphi)|^{-1} = |\sin\Delta|^{-1}.$$

4.1.2 Local wavelet transform

The wavelet transform at φ then reads as follows:

$$\begin{aligned} \mathcal{W}_f(\varphi, a) &= \int_0^{2\pi} \overline{\psi_a^{(\varphi)}(\alpha)}\, f(\alpha)\, d\alpha \qquad (4.6) \\ &= \int_0^{2\pi} \lambda(a, \alpha)^{1/2}\, \overline{\psi^{(\varphi)}\big(\arcsin\big(a^{-1}\sin(\alpha - \varphi)\big) + \varphi\big)}\, f(\alpha)\, d\alpha. \end{aligned}$$

In this particular case, we have a nice group of translations acting on the circle, so that we can write any locally defined function $\psi^{(\varphi)}$ as

$$\psi^{(\varphi)}(\alpha) = \psi(\alpha - \varphi).$$

Acting with $D_\varphi(a)$ on this function yields a simpler expression for the dilation. Namely, combining (4.5) and (4.4), we get immediately

$$\psi_a^{(\varphi)} = \psi_a(\alpha - \varphi).$$

Inserting this expression in (4.6) we see that the continuous wavelet transform takes the familiar form of a convolution between the signal f and the dilated wavelet:

$$\mathcal{W}_f(\varphi, a) = \int_0^{2\pi} d\alpha \left(\frac{\cos(\alpha - \varphi)}{\sqrt{a^2 - \sin^2(\alpha - \varphi)}} \right)^{1/2} \overline{\psi\big(\arcsin\big(a^{-1}\sin(\alpha - \varphi)\big)\big)}\, f(\alpha). \tag{4.7}$$

4.1.3 Admissibility condition and reconstruction

We impose the following form for the reconstruction integral, to be understood in the strong sense:

$$A_\psi f(\alpha) = \int_0^{2\pi} d\varphi \int_0^{a_\psi(\varphi)} \frac{da}{a^2}\, \mathcal{W}_f(\varphi, a)\, \psi_a(\alpha - \varphi). \tag{4.8}$$

The following theorem shows that the operator A_ψ is actually a simple Fourier multiplier.

Theorem 4.1 (Admissibility condition) *Let $\psi \in \mathfrak{H}$ and m, M two constants such that, for all $n \in \mathbb{Z}$, one has*

$$0 < \mathsf{m} \leqslant \mathcal{A}_\psi(n) = \int_0^{a_\psi(\varphi)} |\widehat{\psi_a}(n)|^2 \frac{da}{a^2} \leqslant \mathsf{M} < +\infty, \tag{4.9}$$

where $\widehat{\psi_a}(n)$ is a Fourier coefficient of ψ_a. Then the linear operator A_ψ defined in (4.8) is bounded with bounded inverse. In other words, the family of wavelets $\{\psi_a^{(\varphi)},\, \varphi \in S^1,\, 0 < a \leqslant a_\psi(\varphi)\}$ is a frame, with frame bounds m, M. More precisely A_ψ is uniquely characterized by the following Fourier multiplier:

$$\widehat{A_\psi}\widehat{f}(n) \equiv \widehat{A_\psi f}(n) = \widehat{f}(n) \int_0^{a_\psi} |\widehat{\psi}_a(n)|^2 \frac{da}{a^2} = \mathcal{A}_\psi(n)\widehat{f}(n).$$

It should be noted that, here as in the standard construction [11], the admissibility condition and the reconstruction formula do *not* depend on the explicit form of dilation chosen. In all cases, the unique ingredient is the dilated wavelet $\psi_a^{(\varphi)}$ and its Fourier coeficients, no matter how the dilation is defined.

4.2 Generalizations

The last remark allows us to treat the case of the two-sphere exactly as in the standard derivation described at length in our previous papers [1, 3] and summarized briefly in Section 3.1 (a). The treatment extends to the n-sphere as well [2].

We may also generalize the treatment of the circle directly, using the vertical projection defined in Section 2.2(a). Indeed, since the two-sphere is invariant under rotation around any axis, the projection process takes place in a section of fixed longitude, that is, a circle. Let us fix the point $\zeta_0 = (\theta_0, \varphi_0) \in \mathbb{S}^2$. Then vertical projection p_{ζ_0} means projection along the axis $O\zeta_0$ onto T_{ζ_0}, the plane tangent at ζ_0. This projection is given by

$$\mathsf{p}_{\zeta_0}(\theta, \varphi) = \big(\sin(\theta - \theta_0), \varphi\big) \in T_{\zeta_0},\ \zeta_0 = (\theta_0, \varphi_0).$$

For instance, if we take $\theta_0 = \pi$ (the usual vertical projection on the plane tangent at the South Pole S), then $\mathsf{p}_{\zeta_0}(\theta, \varphi) = (\sin\theta, \varphi)$ (in polar coordinates in the tangent plane T_S). The corresponding formula for an arbitrary point $\zeta_0 = (\theta_0, \varphi_0)$ may be obtained by performing a rotation of θ_0 around the axis Ox, but the result is not illuminating.

This being said, there remains an open problem, namely, how to go from a local WT to a global one. In other words, how can we go from one point to another one on $\mathcal{M}$. In the language of differential geometry, this means going from one local chart to the next one, and the tools for that are available. For example, in the case of the sphere $\mathbb{S}^2$ (or the circle), one needs two charts, one for each hemisphere, with an overlap around the equator, a well-known problem familiar to physicists of the 1970s in the context of a proper treatment of magnetic monopoles, for instance. Clearly, some work remains to be done here on the wavelet side.

5 Lifting the DWT onto $\mathcal{M}$

5.1 Lifting the DWT onto $\dot{\mathbb{S}}^2$ by inverse stereographic projection

The same technique of lifting a wavelet transform from a tangent plane to the manifold $\mathcal{M}$, by a suitable inverse projection, may be applied to the discrete WT. In this way, one can obtain orthonormal wavelet bases on $\mathcal{M}$, locally or globally, depending on the projection used. We illustrate this technique first for the case of the pointed two-sphere $\dot{\mathbb{S}}^2$ with the stereographic projection from the North Pole.

In the notations of Section 2.1(a), we know that the stereographic projection p induces a unitary map $\pi : L^2(\dot{\mathbb{S}}^2) \to L^2(\mathbb{R}^2)$ with inverse

$$(\pi^{-1}F)(\zeta) = F^s(\zeta) := \nu(\zeta)F(\mathsf{p}(\zeta)), \text{ for all } F \in L^2(\mathbb{R}^2),$$

i.e., $F^s = \nu \cdot (F \circ \mathsf{p}) \in L^2(\dot{\mathbb{S}}^2)$, and one has

$$\langle F, G\rangle_{L^2(\mathbb{R}^2)} = \langle F^s, G^s\rangle_{L^2(\dot{\mathbb{S}}^2)}, \ \forall\, F, G \in L^2(\mathbb{R}^2),$$

which is the particularization of (2.2) to $\dot{\mathbb{S}}^2$. Therefore, F, G are orthogonal in $L^2(\mathbb{R}^2)$ if and only if F^s, G^s are orthogonal in $L^2(\dot{\mathbb{S}}^2)$.

Now consider the DWT in the tangent plane. Start from a 2-D plane multiresolution analysis (MRA)

$$\ldots \subset \mathbf{V}_{-2} \subset \mathbf{V}_{-1} \subset \mathbf{V}_0 \subset \mathbf{V}_1 \subset \mathbf{V}_2 \subset \ldots$$

Taking for simplicity the tensor product scaling function $(\mathbf{x}) = \phi(x)\phi(y)$, one gets

$$\mathbf{V}_{j+1} = \mathbf{V}_j \oplus \mathbf{W}_j$$

where $\mathbf{W}_j$ has an orthonormal basis generated by the three wavelets

$${}^h\Psi(x, y) = \phi(x)\psi(y), \quad {}^v\Psi(x, y) = \psi(x)\phi(y), \quad {}^d\Psi(x, y) = \psi(x)\psi(y).$$

For any $F \in L^2(\mathbb{R}^2)$, write

$$F_{j,\mathbf{k}}(x, y) := 2^j F(2^j x - k_1, 2^j y - k_2), \ j \in \mathbb{Z}, \ \mathbf{k} = (k_1, k_2) \in \mathbb{Z}^2.$$

Then $\{{}^\lambda\Psi_{j,\mathbf{k}},\ \mathbf{k} = (k_1, k_2) \in \mathbb{Z}^2,\ \lambda = h, v, d\}$ is an orthonormal basis for $\mathbf{W}_j$ and $\{{}^\lambda\Psi_{j,\mathbf{k}},\ j \in \mathbb{Z}$, $\mathbf{k} \in \mathbb{Z}^2,\ \lambda = h, v, d\}$ is an orthonormal basis for $\overline{\bigoplus_{j\in\mathbb{Z}} \mathbf{W}_j} = L^2(\mathbb{R}^2)$.

Next, we lift everything onto $\dot{\mathbb{S}}^2$ by p^{-1}. For $j \in \mathbb{Z}$, define $\mathcal{V}^j := \{\nu \cdot (F \circ \mathsf{p}),\ F \in \mathbf{V}^j\}$, where $\{\mathbf{V}^j,\ j \in \mathbb{Z}\}$ is the 2-D plane multiresolution analysis. Then $\mathcal{V}^j \subset \mathcal{V}^{j+1}$ for $j \in \mathbb{Z}$, $\mathcal{V}^j$ are closed subspaces of $L^2(\dot{\mathbb{S}}^2)$ and one has

$$\bigcap_{j\in\mathbb{Z}} \mathcal{V}^j = \{0\}, \qquad \overline{\bigcup_{j\in\mathbb{Z}} \mathcal{V}^j} = L^2(\dot{\mathbb{S}}^2).$$

If $\{\Phi_{0,\mathbf{k}},\ \mathbf{k} \in \mathbb{Z}^2\}$ is an orthonormal basis of V^0, then $\{\Phi^s_{0,\mathbf{k}},\ \mathbf{k} \in \mathbb{Z}^2\}$ is an orthonormal basis of $\mathcal{V}^0$. In other words, $(\mathcal{V}^j)_{j\in\mathbb{Z}}$ is a multiresolution analysis of $L^2(\dot{\mathbb{S}}^2)$.

As usual, define the wavelet spaces $\mathcal{W}^j = \mathcal{V}^{j+1} \ominus \mathcal{V}^j$. Then $\{{}^\lambda\Psi^s_{j,\mathbf{k}},\ \mathbf{k} \in \mathbb{Z}^2,\ \lambda = h, v, d\}$ is an orthonormal basis of $\mathcal{W}^j$ and $\{{}^\lambda\Psi^s_{j,\mathbf{k}},\ j \in \mathbb{Z},\ \mathbf{k} \in \mathbb{Z}^2,\ \lambda = h, v, d\}$ is an orthonormal basis of $\overline{\left(\bigoplus_{j\in\mathbb{Z}} \mathcal{W}_j\right)} = L^2(\dot{\mathbb{S}}^2)$.

It follows that all the features of the plane WT are transported to the spherical WT. If Φ has compact support in $\mathbb{R}^2$, then $\Phi^s_{j,\mathbf{k}}$ has local support on $\dot{\mathbb{S}}^2$ (indeed, the 'diameter' of $\operatorname{supp}\Phi^s_{j,\mathbf{k}}$ tends to 0 as $j \to \infty$). An orthonormal 2-D wavelet basis yields an orthonormal spherical wavelet basis. Smooth 2-D wavelets yield smooth spherical wavelets. In particular, Daubechies wavelets yield locally supported and orthonormal wavelets on $\dot{\mathbb{S}}^2$. Thus the same tools as in the planar 2-D case can be used for the decomposition and reconstruction matrices, so that existing toolboxes may be used. Further details and examples may be found in [29].

A similar construction may be performed for the other conic sections, the upper sheet of the two sheeted hyperboloid $\mathbb{H}^2$ (using any of the conical projections described in Section 2.3 or the vertical projection, since the stereographic projection is somewhat pathological) and the paraboloid (using the vertical projection).

5.2 Building a DWT on $\mathbb{S}^2$ by radial projection

An alternative that has proven to be remarkably efficient is to design a DWT on the sphere by radial projection from the faces of a convex polyhedron, as described in Section 2.4 [23, 27].

Let again Γ be a convex polyhedron with triangular faces, containing the origin in its interior. The idea of the method is to obtain wavelets on $\mathbb{S}^2$ first by moving planar, compactly supported, wavelets to the faces of Γ and then projecting them radially onto $\mathbb{S}^2$. Using this technique, one may obtain the following results:

(1) Piecewise constant orthogonal wavelet bases on the faces of Γ yield piecewise constant wavelet bases on spherical triangulations [24]. Here the orthogonality is with respect to the scalar product $\langle \cdot, \cdot \rangle_\Gamma$, not the usual scalar product in $L^2(\mathbb{S}^2)$, but the main advantage is that the matrices used in decomposition and reconstruction are orthogonal and sparse.

(2) Locally supported piecewise linear wavelet bases on triangulations of $\mathbb{R}^2$ yield piecewise rational semi-orthogonal wavelet bases on $\mathbb{S}^2$, having local support and satisfying the Riesz stability property, hence continuous [23].

(3) Wavelets on $\mathbb{S}^2$, taking a cube for Γ and wavelets on an interval [26].

In addition, the method can be extended to the construction of wavelets on sphere-like surfaces (closed surfaces obtained by a smooth deformation of $\mathbb{S}^2$) [25].

6 A continuous wavelet transform on graphs

As ultimate step of our analysis, we consider the case of a WT on a graph. A *graph* is a mathematical object that is well suited to model pairwise relations between objects of a certain collection, such as the nodes of a sensor network or points sampled out of a surface or manifold. A graph can thus be defined as a collection V of vertices or nodes and a collection E of edges that connect pairs of vertices. We shall only consider finite graphs, hence both sets will be finite. A graph may be *undirected*, when there is no distinction between the two endpoints of each edge, or *directed* if edges carry a notion of direction, i.e., the edge from vertex a to vertex b is distinguished from the edge from vertex b to vertex a. We shall consider undirected graphs only. Another way of defining an (undirected) graph is provided by its *adjacency matrix* A, that is, a square matrix $A = (a_{ij})_{i,j}$ of dimension $d = |V|$, whose entry a_{ij} equals the number of edges between vertex i and vertex j. In the sequel, we will use the notation $i \sim j$ to denote that vertices i and j are linked by an edge. For undirected graphs, the adjacency matrix is of course symmetric. A *walk* is a sequence of vertices $v_1, v_2, \ldots, v_k$ such that $v_l v_{l+1}$ is an edge, for $l = 1, 2, \ldots, k-1$. The walk is called a *path* if no vertex (and therefore no edge) is repeated. There is a natural notion of distance between any two vertices, namely, the length of the shortest path between them. It is well-known that the (i, j) entry of the matrix A^n equals the number of walks of length n between vertices i and j.

In the sequel, we will assume that our signals of interest are functions $f : V \to \mathbb{R}$, which can be identified with d-dimensional real vectors $f \in \mathbb{R}^d$. We want to design a wavelet transform on the graph. In particular, we would like that the scaling parameter of the wavelet be in accordance with the notion of distance between vertices. Several approaches to this problem have already been considered, although with quite different mathematical formulations and properties:

- In [13], simple compactly supported wavelets are constructed using the hop distance neighborhoods on graphs and applied to Internet traffic data. This construction is purely discrete and does not involve spectral arguments. Moreover there is no generic reconstruction formula.

- Diffusion wavelets [12] form an orthogonal basis of wavelet-like functions on a graph. The construction partly shares our idea of using the spectral domain induced by the Laplacian operator, but is then quite constrained by the orthogonality requirement.

Our construction depends on two fundamental ingredients. First, a suitable notion of Fourier transform on the graph, that will be used to construct explicitly a scaling. Then, we will need a way to localize wavelets around any chosen vertex of the graph. The key notion for both steps is the fundamental object of spectral graph theory, namely, the *Laplacian matrix*. In our finite dimensional, undirected setting, the Laplacian is defined as the matrix L with entries

$$\ell_{i,j} = \begin{cases} \deg(i), & \text{if } i = j, \\ -1, & \text{if } i \neq j \text{ and } i \sim j, \\ 0, & \text{otherwise,} \end{cases} \tag{6.1}$$

where $\deg(i)$, the degree of i, is the number of edges incident to i. The Laplacian is known to be a positive semi-definite matrix. Thus it has a well-defined eigendecomposition. We will denote by λ_k and $\phi_k = (\phi_k(i))_{i=1,\dots,d}$, $k = 0, \dots, d-1$, its eigenvalues and corresponding eigenvectors, respectively. We order the eigenvalues in increasing order, $\lambda_0 \leqslant \lambda_1 \leqslant \dots \leqslant \lambda_{d-1}$. Note that we always have $\lambda_0 = 0$. For simplicity, we consider that no eigenvalue is degenerate, but this assumption can easily be relaxed. The eigenvectors form an orthonormal system that we can use to decompose any signal (in the case of degenerate eigenvalues, this can always be enforced). They will play essentially the same role as traditional Fourier modes, which are also defined as eigenfunctions of the Laplacian. The Fourier coefficients of $f \in \mathbb{R}^d$ are defined as $\widehat{f}_m = \langle \phi_m, f \rangle$, with the traditional Euclidean scalar product.

The Laplacian eigenfunctions can be used to define a class of operator valued functions via their spectral decomposition (this is called the *Borel functional calculus*). Let $\psi : \mathbb{R}^+ \to \mathbb{R}$ be a square integrable function. Define the operator valued function $\Psi(L)$ by its action on functions on V:

$$\Psi(L)f = \sum_{k=0}^{d-1} \psi(\lambda_k)\, \widehat{f}_k\, \phi_k, \text{ for } f \in \mathbb{R}^d.$$

For instance, choosing $\psi(u) = u$, we recover the spectral decomposition of the Laplacian:

$$Lf = \sum_{k=0}^{d-1} \lambda_k\, \widehat{f}_k\, \phi_k.$$

With a slight abuse of language, we will call $\psi(\lambda_k)$ the Fourier transform of the operator Ψ, a statement meaning that $\psi(\lambda_k)\widehat{f}_k$ are the Fourier coefficients of the function $\Psi(L)f$. Using this analogy, the class of operators we consider are thus Fourier multipliers. In our finite dimensional setting, $\Psi(L)$ is simply a $d \times d$ matrix. Using this indirect description, it is natural to dilate the operator-valued function $\Psi(L)$ by properly scaling its Fourier coefficients:

$$\big(\Psi(tL)f\big)(j) = \sum_{k=0}^{d-1} \psi(t\lambda_k)\, \widehat{f}_k\, \phi_k(j),\ t \in \mathbb{R}^+_*,\ j = 1, \ldots, d.$$

This idea, originally due to Holschneider [18] and Freeden [14], has been revived in the context of spherical wavelets [21, 30, 32] and the so-called *needlets* [22]. Of particular interest to us is the case where the signal of interest is a Kronecker delta at vertex i:

$$\big(\Psi(tL)\delta_i\big)(j) = \sum_{k=0}^{d-1} \psi(t\lambda_k)\phi_k(i)\phi_k(j).$$

We will interpret this equation as the definition of a function of scale t and localized at vertex i. Both operations, scaling and localization, depend on ψ, that we call a generator. By using these mechanisms at various scales and for all vertices of the graph, we construct a family of functions, $\{\psi_{i,t} : V \to \mathbb{R}\}$, indexed by scale and location, namely,

$$\psi_{i,t} := \Psi(tL)\delta_i, \quad i \in V,\, t \in \mathbb{R}^+_*, .$$

It is natural to call wavelets such localized and scaled functions and, by extension, we can formally define the wavelet transform of a function $f : V \to \mathbb{R}$ as the set of coefficients

$$\begin{aligned} \mathcal{W}^{\psi}_f(i,a) &= \langle \psi_{i,a}, f\rangle \\ &= \sum_{j \in V} \big(\psi_{i,a}\big)(j) f(j). \end{aligned}$$

For a genuine wavelet transform, we still need an inversion formula. Intuitively, it should take the following form:

$$f = c_\psi^{-1} \sum_{i \in V} \int_{\mathbb{R}^+_*} \frac{da}{a^\beta}\, \mathcal{W}^{\psi}_f(i,a)\, \psi_v, \tag{6.2}$$

where β is an arbitrary weight. The characterization of generators that allow for such a general inversion is given by the following result.

Theorem 6.1 (Graph Wavelet Generator) *Let $\psi \in L^2(\mathbb{R}^+)$ and c_ψ be a constant such that*

$$0 < c_\psi = \int_0^{+\infty} |\psi(a)|^2\, \frac{\mathrm{d}a}{a^\beta} < +\infty. \tag{6.3}$$

Then the reconstruction formula (6.2) *holds true for any $f \in \mathbb{R}^d$.*

The proof is a trivial application of the spectral decomposition of L. Note that we recover a condition which is very reminiscent of the classical wavelet admissibility condition. In particular, the condition is satisfied whenever the generator ψ is a continuous function that vanishes at the origin, i.e., $\psi(0) = 0$, which implies

$$\sum_{j \in V} \big(\Psi(tL)\delta_i\big)(j) = 0, \forall\, t \in \mathbb{R}^+_*,\, i \in V.$$

An admissible wavelet ψ is thus a zero mean, or more generally oscillating, function associated to the graph. Note as well that it is absolutely trivial to construct admissible wavelet generators. In particular, Euclidean wavelets can be used as generators.

Links with the traditional continuous wavelet transform can be drawn much further. Consider $\mathbb{Z}$ as the set of vertices, with edges of unit length connecting any vertex (integer number) to its two nearest neighbours. One easily checks that the Laplacian is just a finite difference approximation to the second derivative and the associated eigenvectors are the normal Fourier modes. In that case, our arguments provide a simple digital wavelet transform with continuous scales, defined in the Fourier domain. Similarities can be observed with other wavelet constructions, at least informally. Indeed, suppose the vertices are sampled from an underlying smooth compact manifold. Then it has been shown in [17, 31] that the Laplacian matrix converges to the matrix representing the Laplace-Beltrami operator on the manifold as one increases the sampling density. In that case, graph wavelets would resemble wavelets on the underlying manifold, more and more closely. This can have significant practical impact to design digital wavelets on sampled manifolds without even having to consider the underlying geometry: it is also automatically embedded in the graph connectivity. Note also that the sampling does not have to be uniform, this construction handles scattered data in a completely natural way. Figure 1 illustrates this construction for an undirected graph made of scattered points in the plane.[4] In this example we have used the following generator (Mexican Hat wavelet):

$$\psi(u) = u^2 e^{-u^2}.$$

References

[1] J-P. Antoine, P. Vandergheynst, Wavelets on the 2-sphere: A group-theoretical approach, Applied Comput. Harmon. Anal. **7** (1999)262–291 .

[2] J-P. Antoine, P. Vandergheynst, Wavelets on the n-sphere and other manifolds, J. Math. Phys. **39** (1998) 3987–4008.

[3] J-P. Antoine, L. Demanet, L. Jacques, P. Vandergheynst, Wavelets on the sphere: Implementation and approximations, Applied Comput. Harmon. Anal. **13** (2002) 177–200.

[4] J-P. Antoine, R. Murenzi, P. Vandergheynst, S.T. Ali, Two-dimensional Wavelets and Their Relatives, Cambridge University Press, Cambridge (UK), 2004.

[5] J-P. Antoine, I. Bogdanova, P. Vandergheynst, The continuous wavelet transform on conic sections, Int. J. Wavelets, Multires. and Inform. Proc.**6**(2007) 137–156.

[6] A. Askari Hemmat, Z. Yazdani Fard, Continuous wavelet transform on the one-sheeted hyperboloid, preprint.

[7] I. Bogdanova, Wavelets on non-Euclidean manifolds, PhD thesis, EPFL, 2005.

[8] I. Bogdanova, P. Vandergheynst, J-P. Antoine, L. Jacques, M. Morvidone, Stereographic wavelet frames on the sphere, Appl. Comput. Harmon. Anal. **26** (2005) 223–252 .

[9] I. Bogdanova, P. Vandergheynst, J-P. Gazeau, Continuous wavelet transform on the hyperboloid, Applied Comput. Harmon. Anal. **23** (2007) 286–306 (2007).

[4]The example is taken from the Matlab BGL toolbox [20]

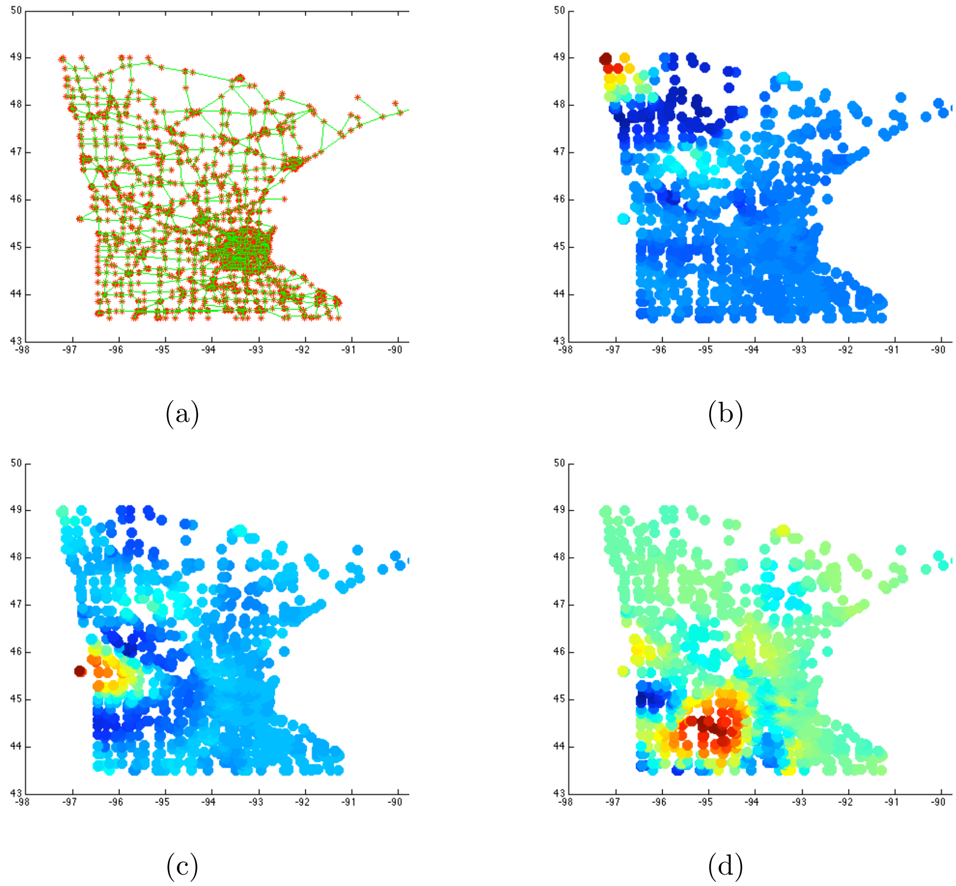

Figure 1: Example of spectral graph wavelets. The original graph (a) with vertices indicated by stars and the edges connecting them. Wavelets localized at different nodes on the graph and at varying scales (b-d).

[10] J. Bros, U. Moschella, Fourier analysis and holomorphic decomposition on the one-sheeted hyperboloid, preprint, arXiv:math-ph/0311052v1 27 Nov 2003.

[11] M. Calixto, J. Guerrero, Wavelet transform on the circle and the real line: A unified group-theoretical treatment, Applied Comput. Harmon. Anal. **21** (2006) 204–229.

[12] R.R. Coifman, M. Maggioni, Diffusion wavelets, Appl. Comput. Harmon. Anal. **21** (1), 53–94 (2006).

[13] M. Crovella, E. Kolaczyk, Graph wavelets for spatial traffic analysis, in Proc. IEEE INFOCOM, (2003).

[14] W. Freeden, U. Windheuser, Combined spherical harmonic and wavelet expansion — A future concept in Earth's gravitational determination, Applied Comput. Harmon. Anal. **4**, 1–37 (1997).

[15] A. Grossmann, J. Morlet, Decomposition of Hardy functions into square integrable wavelets of constant shape, SIAM J. Math. Anal., **15** (1984) 723–736 (1984).

[16] C. Heil, D.F. Walnut (Eds.), Fundamental Papers in Wavelet Theory, Princeton University Press, Princeton, NJ, 2006.

[17] M. Hein, J. Audibert, U. von Luxburg, From graphs to manifoldsWeak and strong pointwise consistency of graph Laplacians, in: Proc. 18th Conf. Learning Theory (COLT), P. Auer, R. Meir, (Eds.), Lecture Notes Comput. Sci., vol. 3559, Springer, Berlin, 2005, pp. 470–485.

[18] M. Holschneider, Continuous wavelet transforms on the sphere, J. Math. Phys. **37**, 4156–4165 (1996).

[19] G. Honnouvo, Gabor Analysis and Wavelet Transforms on some Non-Euclidean 2-Dimensional Manifolds, PhD thesis, Concordia Univ., Montreal, PQ, Canada, 2007; and private communication.

[20] Matlab-BGL is a Matlab graph library, due to D. Gleich, available at the Stanford website `http://www.stanford.edu/∼dgleich/programs/matlab_bgl/`.

[21] J.D. McEwen, M.P. Hobson, A.N. Lasenby, A directional continuous wavelet transform on the sphere, arXiv:astro-ph/0609159 v1, Sep. 2006 .

[22] F.J. Narcowich, P. Petrushev, J.D. Ward, Localized tight frames on spheres, SIAM Journal of Mathematical Analysis, **38** (2), 574594 (2006).

[23] D. Roşca, Locally supported rational spline wavelets on the sphere, Math. Comput., **74** (252), 1803–1829 (2005).

[24] D. Roşca, Haar wavelets on spherical triangulations, in Advances in Multiresolution for Geometric Modelling, N.A. Dogson, M.S. Floater, M.A. Sabin (Eds.), Springer, Berlin, 2005, pp. 407–419.

[25] D. Roşca, Piecewise constant wavelets defined on closed surfaces, J. Comput. Anal. Appl. **8**(2), 121–132 (2006).

[26] D. Roşca, Weighted Haar wavelets on the sphere, Int. J. Wavelets, Multiresolut. and Inf. Process., **5** (3), 501–511 (2007).

[27] D. Roşca, Wavelet bases on the sphere obtained by radial projection, J. Fourier Anal. Appl., **13** (4), 421-434 (2007).

[28] D. Roşca, On a norm equivalence on $L^2(S^2)$ to appear in Results Math. (2009)

[29] D. Roşca, J-P. Antoine, Locally supported orthogonal wavelet bases on the sphere via stereographic projection, preprint (2008).

[30] J.L. Sanz, D. Herranz, M. López-Caniego, F. Argüeso, Wavelets on the sphere. Application to the detection problem, arXiv:astro-ph/0609351 v1, Sep. 2006.

[31] A. Singer, From graph to manifold Laplacian: The convergence rate, Appl. Comput. Harmon. Anal. **21** 128–134 (2006).

[32] Y. Wiaux, J.D. McEwen, P. Vandergheynst, O. Blanc, Exact reconstruction with directional wavelets on the sphere, Mon. Not. R. Astron. Soc., **388**, 770 (2008).

[33] Y. Wiaux, L. Jacques, P. Vandergheynst, Correspondence principle between spherical and Euclidean wavelets, Astrophys. J., **632**, 15–28 (2005).